6.5

TOP-OF-ATMOSPHERE RADIATION BUDGET OVER SNOW AND SEA ICE SURFACES DERIVED FROM CERES MEASUREMENTS

Seiji Kato*
Center for Atmospheric Sciences
Hampton University, Hampton, Virginia

1. Introduction

Clouds and the Earth's Radiant Energy System (CERES, Wielicki et al. 1996) instruments on *Terra* are taking measurements of broadband shortwave, total, and window radiances since March 2000. Because the CERES instruments can be operated under the rotating azimuth mode, they can take radiance measurements over snow covered surface from a wide range of viewing angles. Angular distribution models (ADM) for snow and sea ice are developed in order to estimate the top-of-atmosphere broadband shortwave, longwave and window irradiance using radiance measurements by CERES instruments. Because of a large difference of the angular dependence of radiances, ADM is divided into three surface types, permanent snow, fresh snow, and sea ice. ADM scene types are further divided using Moderate Resolution Imaging Spectrometer (MODIS) derived properties (Minnis et al. 2003). This paper briefly describes the method of building empirical shortwave, longwave and window snow angular distribution models that can be used to derive the irradiance from radiance measurements. General descriptions of Terra ADMs are given in Loeb et al. (2004) and detail descriptions of snow and sea ice ADMs are give in Kato et al. (2004). An analysis using the shortwave and longwave irradiance is also presented in this paper.

2. Shortwave Angular Distribution Model

CERES footprints that contain snow or sea ice are divided into three surface types, permanent snow, fresh snow, and sea ice, using surface types defined by International Geosphere-Biosphere Programme (IGBP) and National Snow and Ice Data Center (NSIDC, Cavalieri et al. 1990, Comiso 1990, Hollinger et al. 1990) daily snow and sea ice maps. Permanent snow includes perennial snow over Antarctica and Grenland ice sheets, glaciers, and ice shelfs. Fresh snow includes seasonal snow over land. Sea ice includes ice in oceans and lakes (Table 1).

Because anisotropy of shortwave radiation field is affected by presence of clouds and snow, we further use the cloud fraction, snow fraction, cloud optical thickness and snow and sea ice brightness to determine angular distribution model scene types (Table 2). These classifications lead to 10 scene types for permanent snow, and 25 scene types for fresh snow and sea ice. To build empirical angular distribution models, we sort the radiance measured by CERES instruments into angular bins. The width of the bin is 5 degree for the viewing zenith angle, 5 degree for the relative azimuth angle and 5 degree for the solar zenith angle (2 degree solar zenith angle for the permanent snow model). We then determine the average radiance $\bar{I}$ and ADM mean irradiance F_{adm} of each scene type. These angular distribution models allow us to estimate the irradiance from each CERES radiance measurement using

$$F = \frac{\pi I}{\langle R \rangle} = \frac{I}{\langle \bar{I} \rangle} \langle F_{adm} \rangle, \tag{1}$$

where I is the instantaneous CERES radiance, R is the anisotropic factor, and $\langle\ \rangle$ indicates the value interpolated at the viewing zenith, relative azimuth, and solar zenith angles of the measurement. Note that $\bar{I}$ and R is a function of scene type in addition to viewing geometry (viewing zenith angle, relative azimuth angle and solar zenith angle).

3. Longwave and Window Angular Distribution Model

Similar to shortwave angular distribution models, longwave models are separated by three surface types. We use the cloud fraction, effective surface temperature, and the effective temperature difference between the surface and cloud top to determine the scene type. These classifications lead to 24 scene types for all three surface types. CERES radiances are sorted into viewing zenith angler bins of which width is 2 degree. Therefore, the longwave and window anisotropic factor is only a function of viewing zenith angle and scene type. Daytime and nighttime models are built from daytime and nighttime data, respectively, using the same scene type classification.

* Corresponding author address: Seiji Kato, Mail Stop 420, NASA Langley Research Center Hampton, VA 23681-2199; e-mail s.kato@larc.nasa.gov.

Table 1: CERES Surface Type Definition

Source	Descriptions
Permanent Snow	
IGBP surface type	Ice sheets
(Loveland and Belward, 1997)	Glaciers
	Ice shelfs
Fresh Snow	
NSIDC and NOAA snow map	Seasonal snow
Imager-derived snow and ice	over land
Sea Ice	
NSIDC and NOAA snow map	Sea ice
Imager-derived snow and ice	Lake ice

Table 2: Snow and Sea Ice Shortwave Angular Distribution Model Scene Types

Cloud Fraction	Snow and Sea Ice Fraction	Cloud Optical Thickness	Snow Brightness
Permanent Snow			
$\leq$ 0.001	-	≤ 10	Dark
0.01 - 0.25		> 10	Bright
0.25 - 0.50			
0.50 - 0.75			
0.75 - 0.999			
$>$ 0.999			
Fresh Snow and Sea Ice			
$\leq$ 0.01	$\leq$ 0.01	≤ 10	Dark
0.01 - 0.25	0.01 - 0.25	> 10	Bright
0.25 - 0.50	0.25 - 0.50		
0.50 - 0.75	0.50 - 0.75		
0.75 - 0.999	0.75 - 0.999		
$>$ 0.99	$>$ 0.99		

Table 3: Snow and Sea Ice Longwave and Window Angular Distribution Model Scene Types

Cloud Fraction	Surface Temperature Fraction	Cloud Top Surface Temperature Difference
$\leq$ 0.001	$<$ 250 K	$<$ 20 K
0.01 - 0.25	$\geq$ 250 K	$\geq$ 20 K
0.25 - 0.50	(Parm. Snow	
0.50 - 0.75	Night	
0.75 - 0.999	$<$ 240 K	
$>$ 0.999	$\geq$ 240 K)	

4. Net Radiation over Sea Ice

To understand the radiative effect of sea ice and clouds at the top of the atmosphere, irradiances derived from sea ice angular distribution models are sorted as a function of solar zenith angle and surface temperature. The reason for using the solar zenith angle and surface temperature is that shortwave and longwave irradiances at the top of the atmosphere are expected to be a strong function of these two variables. Figures 1 and 2 show, respectively, the clear-sky and all-sky albedo, longwave irradiance, and net irradiance at the top of the atmosphere over sea ice surfaces. Four years of data taken over Arctic from March, April, and May are used to plot Figures 1 and 2. The net radiation is defined as the absorbed shortwave irradiance by the earth minus the outgoing longwave irradiance so that the negative value indicates an energy loss by the earth. As we expect, the clear-sky albedo decreases quickly when surface temperature increases above 270 K, which decreases the sea ice fraction (Figure 3). The net irradiance also changes when the surface temperature increases from 270 K to 280 K, indicating that melting sea ice strongly affects the net irradiance at the top of the atmosphere.

The cloud fraction increases with surface temperature (Figure 3). Clouds increases the albedo over sea ice surfaces even when sea ice cover is nearly 100% (Figures 1 and 2). Clouds reduce the top-of-atmosphere longwave irradiance because effective temperature of clouds is, on average, less than that of sea ice surfaces. Therefore, clouds reduces energy inputs by shortwave as well as energy loss by longwave. As a consequence, the net effect of clouds over sea ice surfaces is small when sea ice cove is 100%. The effect of clouds to the net irradiance is larger when the sea ice cover is less than 100%.

Figure 2 also shows that when the solar zenith angle is greater than 70°, the net irradiance is almost always negative. When the sea ice coverage is larger than 50%, presence of clouds reduces the net irradiance by 10 to 20 Wm^{-2} depending on the surface temperature. Figure 4 shows the effect of clouds on the net irradiance more clearly for a given solar zenith angle and surface temperature. The solar zenith angle range for the plot is between 70° and 75° and surface temperature range is between 270 K and 275 K. Under these solar zenith and surface temperature ranges, clouds reduce the net irradiance at the top of the atmosphere by approximately $20\mathrm{Wm}^{-2}$ when the sea ice cover is nearly 100%. When the sea ice cover is less than approximately 50%, the net effect is approximately $50\mathrm{Wm}^{-2}$.

5. Summary

Snow and sea ice angular distribution models are developed to estimate the irradiance from radiance measurements. Collocation of imager radiances, which are used for scene identifications, with CERES footprints allows us to build scene type dependent angular distribution models. An analysis of top-of-atmosphere shortwave and longwave irradiances indicates that sea ice cover strongly affects the net irradiance. On average, clouds reduce the net irradiance when they are present over sea ice surfaces. The clouds effect is larger when the sea ice cover is small. The effect decreases as increasing the sea ice cover. When the solar zenith angle is larger than approximately 70°, the net irradiance over sea ice surfaces under both clear and all-sky conditions is negative.

Acknowledgments

I thank B. A. Wielicki and N. G. Loeb for useful discussions. The work is supported by the Clouds and the Earth's Radiant Energy System (CERES) project under NASA grant (NNL04AA26G).

References

Cavalieri, D., P. Gloerson, and J. Zwally; DMSP SSM/I daily polar gridded sea ice concentrations. Edited by J. Maslanik and J. Stroeve. Boulder, CO: National Snow and Ice Data Center. Digital media, 1990.

Comiso, J.; DMSP SSM/I daily polar gridded sea ice concentrations. Edited by J. Maslanik and J. Stroeve. Boulder, CO: National Snow and Ice Data Center. Digital media, 1990.

Hollinger, J.P., J.L. Peirce, and G.A. Poe, 1990: SSM/I instrument evaluation, *IEEE Trans. Geosci. Remote Sens. Environ.*, **28**, 781-790.

Kato, S., and N. G. Loeb, 2004: Top-of-atmosphere shortwave broadband observed radiance and estimated irradiance over polar regions from Clouds and the Earth's Radiant Energy System (CERES) instruments on Terra, Submitted to *J. Geophys. Res.*

Loeb, N. G., S. Kato, K. Loukachine, and N. M. Smith, 2004: Angular Distribution Models for Top-of-Atmosphere Radiative Flux Estimation from the Clouds and the Earth's Radiant Energy System Instrument on the Terra Satellite. Part I: Methodology, *J. Atmos. Oceanic Technol,* In press.

Loveland, T. R., and A. S. Belward, 1997: The international Geosphere Biosphere Programme Data and Information System Global Land Cover dataset (DISCover), *Acta Astronaut.,* **41**, 681-689.

Minnis, P., D. F. Young, S. Sun-Mack, P. W. Heck, D. R. Doelling, and Q. Trepte: CERES Cloud Property Retrievals from Imagers on TRMM, Terra, and Aqua, *Proc. SPIE 10th International Symposium on Remote Sensing*, Conference on Remote Sensing of Clouds and the Atmosphere VII, Barcelona, Spain, September 8-12, 37-48, 2003.

Wielicki, B. A., B. R. Barkstrom, E. F. Harrison, B. B. Lee III, G. Louis Smith, and J. E. Cooper: Clouds and the Earth's radiant energy system (CERES); an earth observing system experiment, *Bull. Amer. Meteor. Soc.,* **77**, 853-868, 1996

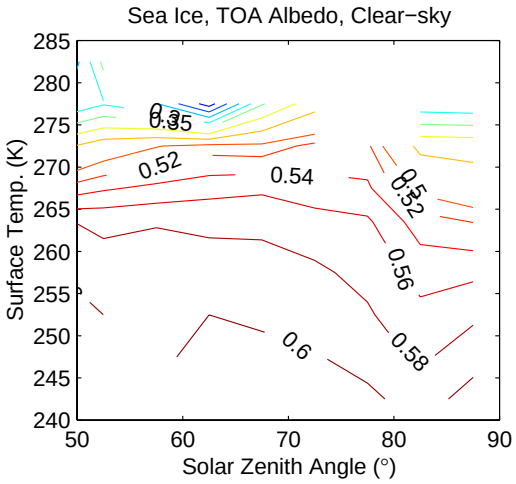

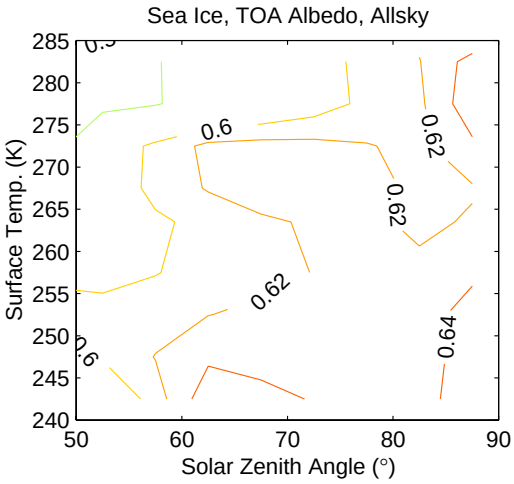

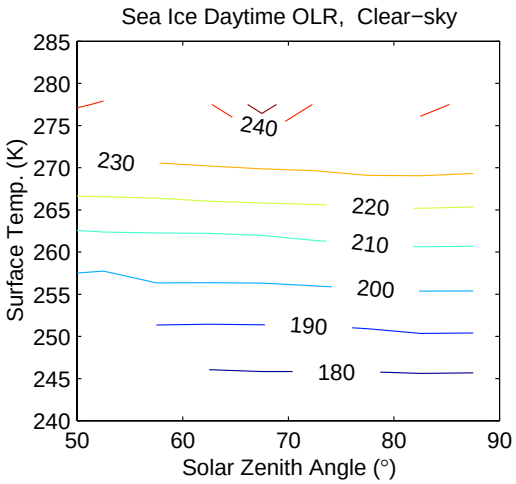

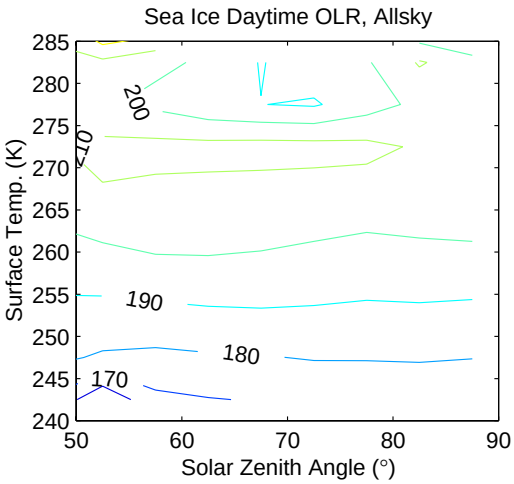

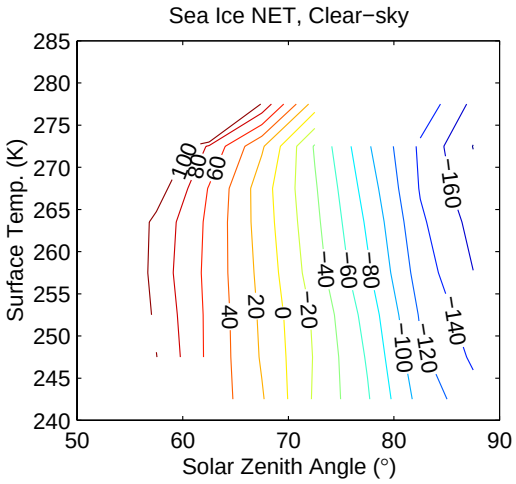

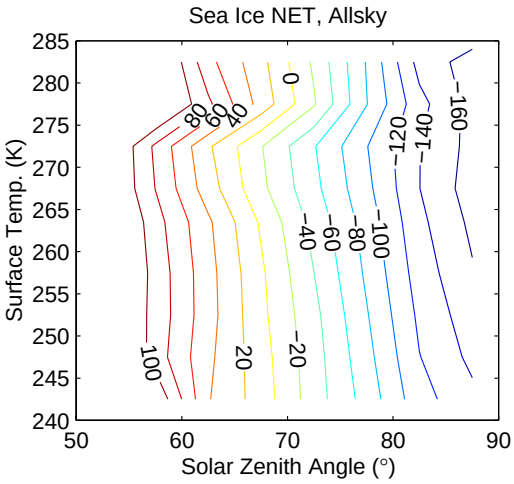

Figure 1 Top-of-atmosphere clear-sky albedo, upward longwave irradiance (in Wm^{-2}), and net irradiance (in Wm^{-2}, positive when energy is deposited to the earth system). These are estimated from radiance CERES measurements taken over sea ice surfaces.

Figure 2 Top-of-atmosphere all-sky albedo, upward longwave irradiance (in Wm^{-2}), and net irradiance (in Wm^{-2}, positive when energy is deposited to the earth system). These are estimated from CERES radiance measurements taken over sea ice surfaces.

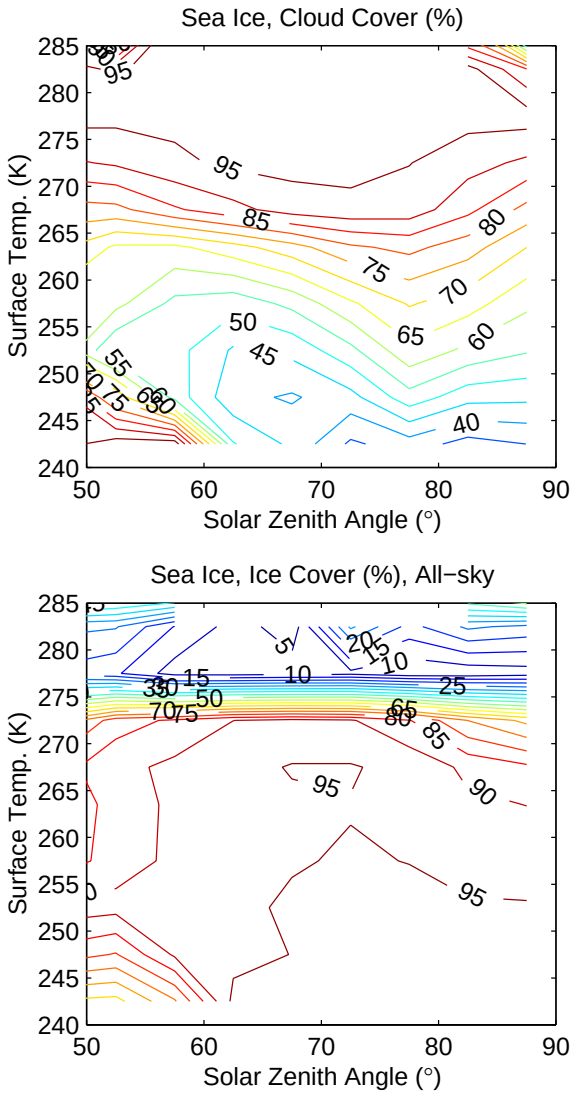

Figure 3 Cloud and sea ice fraction as a function of solar zenith angle and surface temperature. Cloud fraction is derived from MODIS (Minnie et al. 2003) and sea ice fraction is derived from microwave instruments (Cavalieri et al. 1990; Comiso 1990, Hollinger et al. 1990). The fractions are computed over a CERES footprint.

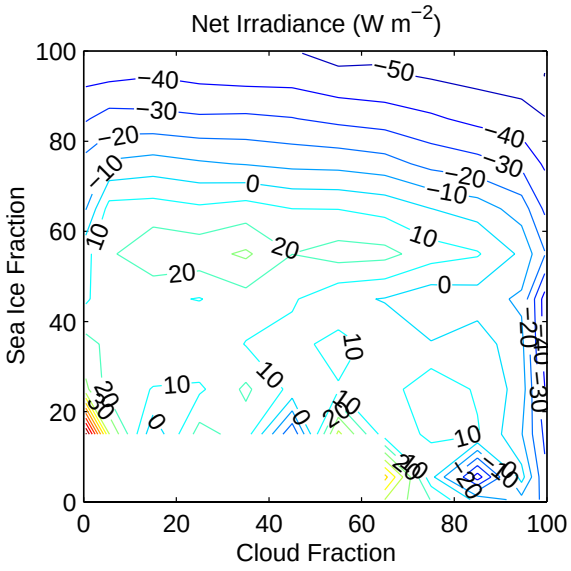

Figure 4 The net irradiance as a function of cloud and sea ice fraction. CERES data taken solar zenith angles between 70° and 75° and surface temperatures between 270 K and 275 K are used for the plot.